

$B^0 \rightarrow \omega\eta^{(\prime)}$ and $\phi\eta^{(\prime)}$ decays in the perturbative QCD approachDong-qin Guo,^{*} Xin-fen Chen,[†] and Zhen-jun Xiao[‡]*Department of Physics and Institute of Theoretical Physics,
Nanjing Normal University, Nanjing, Jiangsu 210097, P.R.China*

(Dated: October 8, 2018)

Abstract

We calculate the branching ratios and CP-violating asymmetries for $B^0 \rightarrow \omega\eta$, $\omega\eta'$, $\phi\eta$ and $\phi\eta'$ decays in the perturbative QCD (pQCD) factorization approach. The pQCD predictions for the CP-averaged branching ratios are $Br(B^0 \rightarrow \omega\eta) = (2.7_{-1.0}^{+1.1}) \times 10^{-7}$, $Br(B^0 \rightarrow \omega\eta') = (0.75_{-0.33}^{+0.37}) \times 10^{-7}$, and $Br(B^0 \rightarrow \phi\eta) = (6.3_{-1.9}^{+3.3}) \times 10^{-9}$, $Br(B^0 \rightarrow \phi\eta') = (7.3_{-2.6}^{+3.5}) \times 10^{-9}$ which are consistent with currently available experimental upper limits. The inclusion of the gluonic contribution can change the branching ratios of $B \rightarrow \omega(\phi)\eta'$ decays by about 10%. The direct CP-violating asymmetries for $B^0 \rightarrow \omega\eta$ and $\omega\eta'$ decays are generally large in size.

PACS numbers: 13.25.Hw, 12.38.Bx, 14.40.Nd

^{*}Electronic address: medongqin@163.com[†]Electronic address: chenxinfen@163.com[‡]Electronic address: xiaozhenjun@njnu.edu.cn

I. INTRODUCTION

As is well-known, the two-body charmless B meson decays provide a good place for testing the standard model (SM) and searching for the new physics signals. Among various $B \rightarrow M_1 M_2$ (here M_i refers to the light pseudo-scalar or vector mesons) decay channels, the decays involving the η or η' meson in the final state have been studied extensively during the past decade because of the so-called $K\eta'$ puzzle or other special features.

In Ref. [1], for example, many decay modes involving $\eta^{(\prime)}$ meson were studied in the QCD factorization (QCDF) approach [2]. In the pQCD factorization approach [3], on the other hand, the $B \rightarrow K\eta^{(\prime)}, \rho\eta^{(\prime)}, \pi\eta^{(\prime)}$ and $\eta^{(\prime)}\eta^{(\prime)}$ decays have been calculated in Refs. [4, 5, 6, 7]. The $B_s \rightarrow (\pi, \rho, \omega, \phi)\eta^{(\prime)}$ decays, furthermore, have also been studied in the pQCD approach [8].

In this paper, we will perform the leading order pQCD calculation for $B \rightarrow \omega\eta^{(\prime)}$ and $\phi\eta^{(\prime)}$ decays. Besides the usual factorizable contributions, we here are able to evaluate the non-factorizable and the annihilation contributions as well. Besides the dominant contributions from the $q\bar{q}$ components of $\eta^{(\prime)}$ mesons, the contribution from the possible gluonic component of $\eta^{(\prime)}$ meson will also be included by using the formulae as given in Ref. [9].

On the experimental side, only the upper limits on the branching ratios of $B \rightarrow \omega(\phi)\eta^{(\prime)}$ decays are available now [10, 11]

$$Br(B^0 \rightarrow \phi\eta) < 0.6 \times 10^{-6}, \quad Br(B^0 \rightarrow \phi\eta') < 1.0 \times 10^{-6}. \quad (1)$$

$$Br(B^0 \rightarrow \omega\eta) < 1.9 \times 10^{-6}, \quad Br(B^0 \rightarrow \omega\eta') < 2.8 \times 10^{-6}. \quad (2)$$

But these decays could be measured with good precision in the forthcoming LHC-b experiments if their decay rates are larger than 10^{-8} .

For $B \rightarrow \omega(\phi)\eta^{(\prime)}$ decays considered here, it is generally believed that the $q\bar{q}$ component of $\eta^{(\prime)}$ meson provide the dominant contribution, but it is still very difficult to calculate reliably the gluonic contribution from the possible gluonic component of $\eta^{(\prime)}$ meson [9, 12]. Of course, great efforts have been made for this problem and some progress have been achieved recently [9, 12] in order to explain the large $B \rightarrow K\eta'$ decay rates. In Ref. [9], for instance, the authors found that the possible gluonic contribution is small for both $B \rightarrow \eta$ and $B \rightarrow \eta'$ form factors [9, 13].

This paper is organized as follows. In Sec. II, we give a brief review for the PQCD factorization approach. In Sec. III, we calculate analytically the related Feynman diagrams and present the various decay amplitudes for the studied decay modes. In Sec. IV, we show the numerical results for the branching ratios and CP asymmetries of $B \rightarrow \omega(\phi)\eta^{(\prime)}$ decays. The summary and some discussions are included in the final section.

II. THE THEORETICAL FRAMEWORK

At present, there exist two popular factorization approaches to calculate the hadronic matrix element $\langle M_1 M_2 | O_i | B \rangle$: the QCDF approach [2] and the pQCD approach [3, 14, 15]. The pQCD approach has been developed earlier from the QCD hard-scattering approach [15]. Some elements of this approach are also present in the QCD factorization approach [1, 2]. The two major differences between these two approaches are (a) the

form factors are calculable perturbatively in pQCD approach, but taken as the input parameters extracted from other experimental measurements in the QCDF approach; and (b) the annihilation contributions are calculable and play an important role in producing CP violation for the considered decay modes in pQCD approach, but it could not be evaluated reliably in QCDF approach. Of course, the assumptions behind the pQCD approach, specifically the possibility to calculate the form factors perturbatively, are still under discussion [16]. More efforts are needed to clarify these problems.

In pQCD approach, the decay amplitude is separated into soft (Φ), hard(H), and harder(C) dynamics characterized by different energy scales (t, m_b, M_W). It is conceptually written as the convolution,

$$\mathcal{A}(B \rightarrow M_1 M_2) \sim \int d^4 k_1 d^4 k_2 d^4 k_3 \text{Tr} [C(t) \Phi_B(k_1) \Phi_{M_1}(k_2) \Phi_{M_2}(k_3) H(k_1, k_2, k_3, t)], \quad (3)$$

where the k_i are the momenta of the light quarks included in each of the mesons, and Tr denotes the trace over Dirac and color indices. $C(t)$ is the Wilson coefficient which results from the radiative corrections at short distance. In the above convolution, $C(t)$ includes the harder dynamics at larger scale than M_B scale and describes the evolution of local 4-Fermi operators from m_W (the W boson mass) down to $t \sim \mathcal{O}(\sqrt{\bar{\Lambda} M_B})$ scale, where $\bar{\Lambda} \equiv M_B - m_b$. The function $H(k_1, k_2, k_3, t)$ is the hard part and can be calculated perturbatively. The function Φ_M is the wave function which describes hadronization of the quark and anti-quark to the meson M . While the function H depends on the process considered, the wave function Φ_M is independent of the specific decay process. Using the wave functions determined from other well measured processes, one can make quantitative predictions here.

Since the b quark is rather heavy, we consider the B meson at rest for simplicity. It is convenient to use light-cone coordinate (p^+, p^-, \mathbf{p}_T) to describe the meson's momenta,

$$p^\pm = \frac{1}{\sqrt{2}}(p^0 \pm p^3), \quad \text{and} \quad \mathbf{p}_T = (p^1, p^2). \quad (4)$$

Using these coordinates the B meson and the two final state meson momenta can be written as

$$P_1 = \frac{M_B}{\sqrt{2}}(1, 1, \mathbf{0}_T), \quad P_2 = \frac{M_B}{\sqrt{2}}(1, r_{\omega(\phi)}^2, \mathbf{0}_T), \quad P_3 = \frac{M_B}{\sqrt{2}}(0, 1 - r_{\omega(\phi)}^2, \mathbf{0}_T), \quad (5)$$

respectively, where $r_{\omega(\phi)}^2 = m_{\omega(\phi)}^2/m_B^2$; and the terms proportional to the ratio $m_{\eta(\prime)}^2/m_B^2$ have been neglected.

For the $B \rightarrow \omega \eta$ decay considered here, only the ω meson's longitudinal part contributes to the decay, its polar vector is $\epsilon_L = \frac{M_B}{\sqrt{2}M_\omega}(1, -r_\omega^2, \mathbf{0}_T)$. Putting the light (anti) quark momenta in the B , ω and η meson k_1 , k_2 , and k_3 , respectively, we can choose

$$k_1 = (x_1 P_1^+, 0, \mathbf{k}_{1T}), \quad k_2 = (x_2 P_2^+, 0, \mathbf{k}_{2T}), \quad k_3 = (0, x_3 P_3^-, \mathbf{k}_{3T}). \quad (6)$$

Then, the integration over k_1^- , k_2^- , and k_3^+ in Eq.(3) will lead to

$$\mathcal{A}(B \rightarrow \omega \eta) \sim \int dx_1 dx_2 dx_3 b_1 db_1 b_2 db_2 b_3 db_3 \cdot \text{Tr} [C(t) \Phi_B(x_1, b_1) \Phi_\omega(x_2, b_2) \Phi_\eta(x_3, b_3) H(x_i, b_i, t) S_t(x_i) e^{-S(t)}], \quad (7)$$

where b_i is the conjugate space coordinate of k_{iT} , and t is the largest energy scale in the function $H(x_i, b_i, t)$. The large logarithms $\ln(m_W/t)$ are included in the Wilson coefficients $C(t)$. The large double logarithms ($\ln^2 x_i$) on the longitudinal direction are summed by the threshold resummation, and they lead to the function $S_t(x_i)$ which smears the end-point singularities on x_i . The last term, $e^{-S(t)}$, is the Sudakov form factor which suppresses the soft dynamics effectively [17]. Thus it makes the perturbative calculation of the hard part H applicable at an intermediate scale, i.e., the M_B scale. We will calculate analytically the function $H(x_i, b_i, t)$ for the considered decays in the first order in an α_s expansion and give the convoluted amplitudes in the next section.

A. Wilson Coefficients

For the $B^0 \rightarrow \omega \eta^{(\prime)}$, $B^0 \rightarrow \phi \eta^{(\prime)}$ decays, the related weak effective Hamiltonian H_{eff} can be written as [18]

$$\mathcal{H}_{eff} = \frac{G_F}{\sqrt{2}} \left[V_{ub} V_{ud}^* (C_1(\mu) O_1^u(\mu) + C_2(\mu) O_2^u(\mu)) - V_{tb} V_{td}^* \sum_{i=3}^{10} C_i(\mu) O_i(\mu) \right], \quad (8)$$

where $C_i(\mu)$ are Wilson coefficients at the renormalization scale μ and O_i are the four-fermion operators. For $b \rightarrow d$ transition, for example, these operators can be written as

$$\begin{aligned} O_1^u &= \bar{d}_\alpha \gamma^\mu L u_\beta \cdot \bar{u}_\beta \gamma_\mu L b_\alpha, & O_2^u &= \bar{d}_\alpha \gamma^\mu L u_\alpha \cdot \bar{u}_\beta \gamma_\mu L b_\beta, \\ O_3 &= \bar{d}_\alpha \gamma^\mu L b_\alpha \cdot \sum_{q'} \bar{q}'_\beta \gamma_\mu L q'_\beta, & O_4 &= \bar{d}_\alpha \gamma^\mu L b_\beta \cdot \sum_{q'} \bar{q}'_\beta \gamma_\mu L q'_\alpha, \\ O_5 &= \bar{d}_\alpha \gamma^\mu L b_\alpha \cdot \sum_{q'} \bar{q}'_\beta \gamma_\mu R q'_\beta, & O_6 &= \bar{d}_\alpha \gamma^\mu L b_\beta \cdot \sum_{q'} \bar{q}'_\beta \gamma_\mu R q'_\alpha, \\ O_7 &= \frac{3}{2} \bar{d}_\alpha \gamma^\mu L b_\alpha \cdot \sum_{q'} e_{q'} \bar{q}'_\beta \gamma_\mu R q'_\beta, & O_8 &= \frac{3}{2} \bar{d}_\alpha \gamma^\mu L b_\beta \cdot \sum_{q'} e_{q'} \bar{q}'_\beta \gamma_\mu R q'_\alpha, \\ O_9 &= \frac{3}{2} \bar{d}_\alpha \gamma^\mu L b_\alpha \cdot \sum_{q'} e_{q'} \bar{q}'_\beta \gamma_\mu L q'_\beta, & O_{10} &= \frac{3}{2} \bar{d}_\alpha \gamma^\mu L b_\beta \cdot \sum_{q'} e_{q'} \bar{q}'_\beta \gamma_\mu L q'_\alpha, \end{aligned} \quad (9)$$

where α and β are the $SU(3)$ color indices; L and R are the left- and right-handed projection operators with $L = (1 - \gamma_5)$, $R = (1 + \gamma_5)$. The sum over q' runs over the quark fields that are active at the scale $\mu = O(m_b)$, i.e., $q' \in \{u, d, s, c, b\}$. For the Wilson coefficients $C_i(\mu)$ ($i = 1, \dots, 10$), we will use the leading order (LO) expressions, although the next-to-leading order (NLO) results already exist in the literature [18]. This is the consistent way to cancel the explicit μ dependence in the theoretical formulae. For the renormalization group evolution of the Wilson coefficients from higher scale to lower scale, we use the formulae as given in Ref. [19] directly. At the high m_W scale, the leading order Wilson coefficients $C_i(M_W)$ are simple and can be found easily in Ref. [18]. In the pQCD approach, the scale t may be larger or smaller than the m_b scale. For the case of $m_b < t < m_W$, we evaluate the Wilson coefficients at t scale using the leading logarithm running equations, as given in Eq.(C1) of Ref. [19]. For the case of $t < m_b$, we then evaluate the Wilson coefficients at t scale by using $C_i(m_b)$ as input and the formulae given in Appendix D of Ref. [19].

B. $\phi - \omega$ mixing and $\eta - \eta'$ mixing

For the physical isoscalars ϕ and ω meson, we use the “ideal” mixing scheme [20]:

$$\phi(1020) = -s\bar{s}, \quad \omega = \frac{1}{\sqrt{2}} [u\bar{u} + d\bar{d}]. \quad (10)$$

Such ideal mixing are supported by the known experimental measurements [20].

For the $\eta - \eta'$ system, there exist two popular mixing basis: the octet-singlet basis and the quark-flavor basis [21, 22]. Here we use the quark-flavor basis [21] and define

$$\eta_q = (u\bar{u} + d\bar{d})/\sqrt{2}, \quad \eta_s = s\bar{s}. \quad (11)$$

The physical states η and η' are related to η_q and η_s through a single mixing angle ϕ ,

$$\begin{pmatrix} \eta \\ \eta' \end{pmatrix} = U(\phi) \begin{pmatrix} \eta_q \\ \eta_s \end{pmatrix} = \begin{pmatrix} \cos \phi & -\sin \phi \\ \sin \phi & \cos \phi \end{pmatrix} \begin{pmatrix} \eta_q \\ \eta_s \end{pmatrix}. \quad (12)$$

The corresponding decay constants $f_q, f_s, f_{\eta}^{q,s}$ and $f_{\eta'}^{q,s}$ have been defined in Ref. [21] as

$$\begin{aligned} \langle 0 | \bar{q}\gamma^\mu \gamma_5 q | \eta_q(P) \rangle &= -\frac{i}{\sqrt{2}} f_q P^\mu, \\ \langle 0 | \bar{s}\gamma^\mu \gamma_5 s | \eta_s(P) \rangle &= -i f_s P^\mu, \end{aligned} \quad (13)$$

$$\begin{aligned} \langle 0 | \bar{q}\gamma^\mu \gamma_5 q | \eta^{(')}(P) \rangle &= -\frac{i}{\sqrt{2}} f_{\eta^{(')}}^q P^\mu, \\ \langle 0 | \bar{s}\gamma^\mu \gamma_5 s | \eta^{(')}(P) \rangle &= -i f_{\eta^{(')}}^s P^\mu, \end{aligned} \quad (14)$$

while the decay constants $f_{\eta}^{q,s}$ and $f_{\eta'}^{q,s}$ are related to f_q and f_s via the same mixing matrix,

$$\begin{pmatrix} f_{\eta}^q & f_{\eta}^s \\ f_{\eta'}^q & f_{\eta'}^s \end{pmatrix} = U(\phi) \begin{pmatrix} f_q & 0 \\ 0 & f_s \end{pmatrix}. \quad (15)$$

The three input parameters f_q, f_s and ϕ in the quark-flavor basis have been extracted from various related experiments [21, 22]

$$f_q = (1.07 \pm 0.02)f_\pi, \quad f_s = (1.34 \pm 0.06)f_\pi, \quad \phi = 39.3^\circ \pm 1.0^\circ, \quad (16)$$

where $f_\pi = 130$ MeV. In the numerical calculations, we will use these mixing parameters as inputs.

Although η and η' are generally considered as a linear combination of light quark pairs $u\bar{u}, d\bar{d}$ and $s\bar{s}$, it should be noted that a gluonic content of η' meson may be needed to interpret the anomalously large branching ratios of $B \rightarrow K\eta'$ and $J/\Psi \rightarrow \eta'\gamma$ [4, 23]. For $B \rightarrow (\rho, \pi)\eta^{(')}$ decays, however, the good agreement between the pQCD predictions [5, 6] and the measured values for their branching ratios suggest that the gluonic contribution of $\eta^{(')}$ meson should be small. In Ref. [9], very recently, the authors calculated the flavor-singlet contribution to the $B \rightarrow \eta^{(')}$ transition form factors from the gluonic content of the $\eta^{(')}$ meson. They found that the gluonic contribution is small for both $B \rightarrow \eta$ and $B \rightarrow \eta'$ form factors.

Of course, more studies are needed to provide a reliable and precision calculation for the gluonic contribution to the final state involving $\eta^{(\prime)}$ meson. For the sake of simplicity, we here firstly neglect the possible gluonic content of η and η' meson, and use the quark-flavor mixing scheme for η and η' meson as defined in Eq. (12). We will calculate the effects of a non-zero gluonic admixture of η' in next section, and treat them as one kind of theoretical uncertainties.

C. Wave Functions

Now we present the wave functions to be used in the integration. For the wave function of the heavy B meson, we take

$$\Phi_B = \frac{1}{\sqrt{2N_c}} [(\not{p}_B + M_B)\gamma_5\phi_B(\mathbf{k}_1)]. \quad (17)$$

Here only the contribution of the Lorentz structure $\phi_B(\mathbf{k}_1)$ is taken into account, since the contribution of the second Lorentz structure $\bar{\phi}_B$ is numerically small [24, 25] and has been neglected. For the distribution amplitude ϕ_B in Eq. (17), we adopt the model

$$\phi_B(x, b) = N_B x^2 (1-x)^2 \exp \left[-\frac{M_B^2 x^2}{2\omega_b^2} - \frac{1}{2}(\omega_b b)^2 \right], \quad (18)$$

where ω_b is a free parameter and we take $\omega_b = 0.4 \pm 0.04$ GeV in numerical calculations, and $N_B = 91.745$ is the normalization factor for $\omega_b = 0.4$. This is the same wave functions as being used in Refs. [19, 24], which is a best fit for most of the measured hadronic B decays.

The wave function for $d\bar{d}$ components of $\eta^{(\prime)}$ meson is given by [4]

$$\Phi_{\eta_{d\bar{d}}}(p, x, \zeta) \equiv \frac{i\gamma_5}{\sqrt{2N_c}} \left[\not{p}\phi_{\eta_{d\bar{d}}}^A(x) + m_0^{\eta_{d\bar{d}}}\phi_{\eta_{d\bar{d}}}^P(x) + \zeta m_0^{\eta_{d\bar{d}}}(\not{p}\not{\eta} - v \cdot n)\phi_{\eta_{d\bar{d}}}^T(x) \right], \quad (19)$$

where p and x are the momentum and the momentum fraction of $\eta_{d\bar{d}}$ respectively, while $\phi_{\eta_{d\bar{d}}}^A$, $\phi_{\eta_{d\bar{d}}}^P$ and $\phi_{\eta_{d\bar{d}}}^T$ represent the axial vector, pseudoscalar and tensor components of the wave function respectively. Following Ref. [4], we here also assume that the wave function of $\eta_{d\bar{d}}$ is same as the π wave function based on SU(3) flavor symmetry. The parameter ζ is either +1 or -1 depending on the assignment of the momentum fraction x . We also assume that the wave function of the $u\bar{u}$ component is the same as the wave function of $d\bar{d}$ based on the isospin symmetry between the up and down quark. For the wave function of the $s\bar{s}$ component, we also use the same form as given in Eq. (19) for $d\bar{d}$ component but with different chiral enhancement and some other changes to be specified later.

The explicit expressions of chiral enhancement scales $m_0^q = m_0^{\eta_{d\bar{d}}} = m_0^{\eta_{u\bar{u}}}$ and $m_0^s = m_0^{\eta_{s\bar{s}}}$ are given by [9]

$$m_0^q \equiv \frac{m_{qq}^2}{2m_q} = \frac{1}{2m_q} [m_\eta^2 \cos^2 \phi + m_{\eta'}^2 \sin^2 \phi - \frac{\sqrt{2}f_s}{f_q} (m_{\eta'}^2 - m_\eta^2) \cos \phi \sin \phi], \quad (20)$$

$$m_0^s \equiv \frac{m_{ss}^2}{2m_s} = \frac{1}{2m_s} [m_{\eta'}^2 \cos^2 \phi + m_\eta^2 \sin^2 \phi - \frac{f_q}{\sqrt{2}f_s} (m_{\eta'}^2 - m_\eta^2) \cos \phi \sin \phi], \quad (21)$$

and numerically

$$m_0^q = 1.07\text{MeV}, \quad m_0^s = 1.92\text{GeV} \quad (22)$$

for $m_\eta = 547.5$ MeV, $m_{\eta'} = 957.8$ MeV, $f_q = 1.07f_\pi$, $f_s = 1.34f_\pi$ and $\phi = 39.3^\circ$.

For the distribution amplitude $\phi_{\eta_q}^A$, $\phi_{\eta_q}^P$ and $\phi_{\eta_q}^T$, we utilize the results for π meson obtained from the light-cone sum rule [26] including twist-3 contributions:

$$\begin{aligned} \phi_{\eta_q(s)}^A(x) = & \frac{3}{\sqrt{2N_c}} f_{q(s)} x(1-x) \left\{ 1 + a_2^{\eta_q(s)} \frac{3}{2} [5(1-2x)^2 - 1] \right. \\ & \left. + a_4^{\eta_q(s)} \frac{15}{8} [21(1-2x)^4 - 14(1-2x)^2 + 1] \right\}, \end{aligned} \quad (23)$$

$$\begin{aligned} \phi_{\eta_q(s)}^P(x) = & \frac{1}{2\sqrt{2N_c}} f_{q(s)} \left\{ 1 + \frac{1}{2} \left(30\eta_3 - \frac{5}{2}\rho_{\eta_q(s)}^2 \right) [3(1-2x)^2 - 1] \right. \\ & + \frac{1}{8} \left(-3\eta_3\omega_3 - \frac{27}{20}\rho_{\eta_q(s)}^2 - \frac{81}{10}\rho_{\eta_q(s)}^2 a_2^{\eta_q(s)} \right) \\ & \cdot [35(1-2x)^4 - 30(1-2x)^2 + 3] \left. \right\}, \end{aligned} \quad (24)$$

$$\begin{aligned} \phi_{\eta_q(s)}^T(x) = & \frac{3}{\sqrt{2N_c}} f_{q(s)} (1-2x) \\ & \cdot \left[\frac{1}{6} + (5\eta_3 - \frac{1}{2}\eta_3\omega_3 - \frac{7}{20}\rho_{\eta_q(s)}^2 - \frac{3}{5}\rho_{\eta_q(s)}^2 a_2^{\eta_q(s)})(10x^2 - 10x + 1) \right], \end{aligned} \quad (25)$$

with the updated Gegenbauer moments [27, 28]

$$\begin{aligned} a_2^{\eta_q(s)} &= 0.115, \quad a_4^{\eta_q(s)} = -0.015, \quad \rho_{\eta_q} = 2m_q/m_{qq}; \\ \rho_{\eta_s} &= 2m_s/m_{ss}, \quad \eta_3 = 0.015, \quad \omega_3 = -3.0. \end{aligned} \quad (26)$$

For $B \rightarrow \omega\eta^{(\prime)}$ and $\phi\eta^{(\prime)}$ decays, only the longitudinal polarized component Φ_V^L for $V = (\omega, \phi)$ will contribute. The wave function Φ_ω^L , for example, can be written as

$$\Phi_\omega^L = \frac{1}{\sqrt{2N_c}} [m_\omega \not{\epsilon}_L \phi_\omega(x) + \not{\epsilon}_L \not{p} \phi_\omega^t(x) + m_\omega I \phi_\omega^s(x)], \quad (27)$$

where the ϵ_L and \mathbf{p} is the polarization vector and the momentum of the ω meson, the first term in above equation is the leading twist wave function (twist-2), while the second and third terms are subleading twist (twist-3) wave functions. For the case of $V = \phi$, its wave function is the same in structure as that defined in Eq. (27), but with different mass and distribution amplitudes.

For the light meson wave function, we neglect the b dependent part, which is not important in numerical analysis. The distribution amplitudes $\phi_\phi(x)$ and $\phi_\phi^{t,s}(x)$ are given by [29]

$$\phi_\phi(x) = \frac{3}{\sqrt{6}} f_\phi x(1-x), \quad (28)$$

$$\phi_\phi^t(x) = \frac{f_\phi^T}{2\sqrt{6}} \left\{ 3(1-2x)^2 + 1.68C_4^{1/2}(1-2x) + 0.69 \left[1 + (1-2x) \ln \frac{x}{1-x} \right] \right\}, \quad (29)$$

$$\phi_\phi^s(x) = \frac{3}{4\sqrt{6}} f_\phi^T \left[3(1-2x)(4.5 - 11.2x + 11.2x^2) + 1.38 \ln \frac{x}{1-x} \right]. \quad (30)$$

For the ω meson wave function, we use [30, 31]

$$\phi_\omega(x) = \frac{3}{\sqrt{6}} f_\omega x(1-x) \left[1 + 0.18 C_2^{3/2} (1-2x) \right], \quad (31)$$

$$\begin{aligned} \phi_\omega^t(x) = \frac{f_\omega^T}{2\sqrt{6}} \{ & 3(1-2x)^2 + 0.3(1-2x)^2 [5(1-2x)^2 - 3] \\ & + 0.21[3 - 30(1-2x)^2 + 35(1-2x)^4] \}, \end{aligned} \quad (32)$$

$$\phi_\omega^s(x) = \frac{3}{2\sqrt{6}} f_\omega^T (1-2x) [1 + 0.76(10x^2 - 10x + 1)]. \quad (33)$$

The relevant Gegenbauer polynomials are defined by [29]

$$C_2^{3/2}(t) = \frac{3}{2} (5t^2 - 1), \quad (34)$$

$$C_4^{1/2}(t) = \frac{1}{8} (35t^4 - 30t^2 + 3). \quad (35)$$

III. PERTURBATIVE CALCULATIONS

In this section, we will calculate and show the decay amplitude for each diagram including wave functions. The hard part $H(t)$ involves the four quark operators and the necessary hard gluon connecting the four quark operator and the spectator quark. We first consider $B \rightarrow \omega\eta$ decay, and then extend the calculation to other decay modes. Analogous to the $B \rightarrow \rho\eta^{(\prime)}$ decays in [5], there are also eight type diagrams contributing to $B \rightarrow \omega\eta$ and $\omega\eta'$ decay, as illustrated in Figure 1.

For $B \rightarrow \omega\eta$ decay, we firstly consider the usual factorizable diagrams 1(a) and 1(b). The operators $O_{1,2}$ and $O_{3,4,9,10}$ are $(V-A)(V-A)$ currents; the sum of their amplitudes is given by

$$\begin{aligned} F_e = & 4\sqrt{2}\pi G_F C_F m_B^4 \int_0^1 dx_1 dx_3 \int_0^\infty db_1 b_3 db_3 \phi_B(x_1, b_1) \\ & \times \{ [(1+x_3)\phi_\eta^A(x_3, b_3) + (1-2x_3)r_\eta(\phi_\eta^P(x_3, b_3) + \phi_\eta^T(x_3, b_3))] \\ & \cdot \alpha_s(t_e^1) h_e(x_1, x_3, b_1, b_3) \exp[-S_{ab}(t_e^1)] \\ & + 2r_\eta \phi_\eta^P(x_3, b_3) \alpha_s(t_e^2) h_e(x_3, x_1, b_3, b_1) \exp[-S_{ab}(t_e^2)] \}. \end{aligned} \quad (36)$$

where the ratio $r_\eta = m_0^\eta/m_B$ with $m_0^\eta = m_0^q$ or m_0^s as defined in Eqs. (20,21); the color factor $C_F = 4/3$, ϕ_B and $\phi_\eta^{A,P,T}$ are the light-cone distribution amplitudes (LCDAs) of the heavy B meson and the light η meson. The functions h_e , the scales t_e^i and the Sudakov factors S_{ab} will be given explicitly in Appendix A.

The operators $O_{5,6,7,8}$ have the structure of $(V-A)(V+A)$. In some decay channels, some of these operators contribute to the decay amplitude in a factorizable way. Since only the vector part of the $(V+A)$ current contributes to the vector meson production, $\langle \eta | V-A | B \rangle \langle \omega | V+A | 0 \rangle = \langle \eta | V-A | B \rangle \langle \omega | V-A | 0 \rangle$, that is

$$F_e^{P1} = F_e. \quad (37)$$

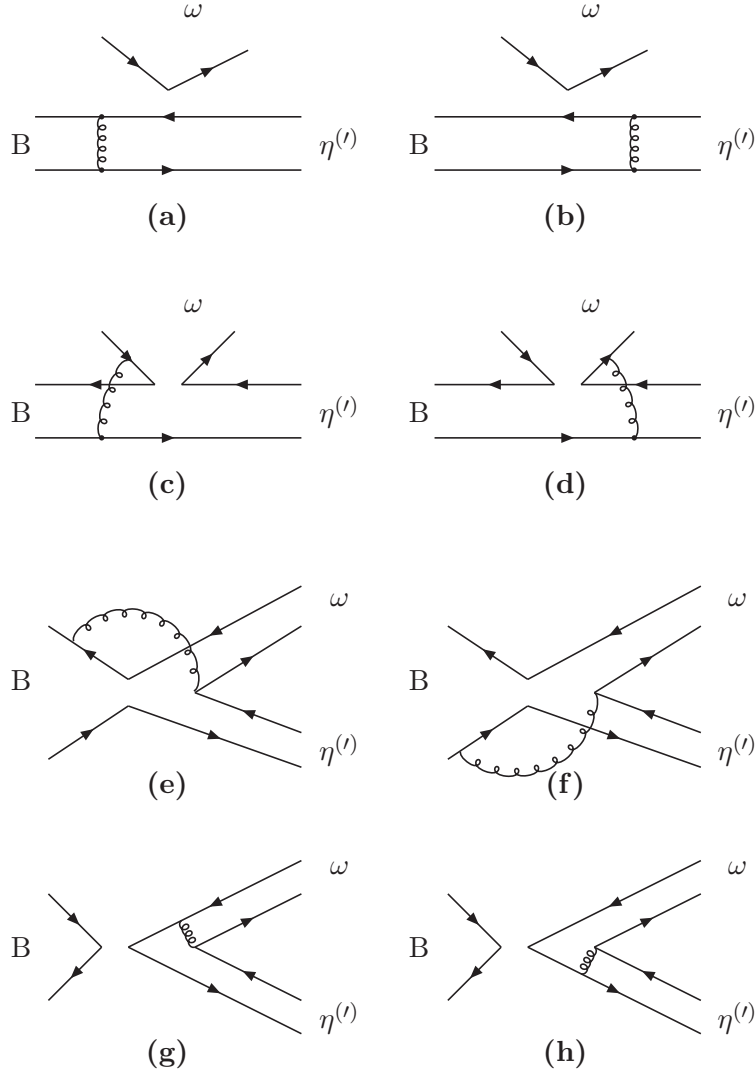


FIG. 1: Feynman diagrams contributing to the $B \rightarrow \omega \eta^{(\prime)}$ decays when the $\eta^{(\prime)}$ meson picks up the spectator quark, where diagram (a) and (b) contribute to the $B \rightarrow \eta^{(\prime)}$ form factor $F_{0,1}^{B \rightarrow \eta^{(\prime)}}$.

For other cases, one needs to do a Fierz transformation for the corresponding operators to get the right flavor and color structure for factorization to work. We may get $(S+P)(S-P)$ operators from $(V-A)(V+A)$ ones. Because neither scalar nor the pseudo-scalar density give contribution to a vector meson production, $\langle \omega | S + P | 0 \rangle = 0$, we get $F_e^{P2} = 0$.

For the non-factorizable diagrams 1(c) and 1(d), all three meson wave functions are involved. The integration of b_3 can be performed using the δ function $\delta(b_3 - b_1)$, leaving only integration of b_1 and b_2 . The decay amplitude for $(V-A)(V-A)$ and $(V-A)(V+A)$

operators can be written as

$$M_e = -M_e^{P2} = \frac{16}{\sqrt{3}} G_F \pi C_F m_B^4 \int_0^1 dx_1 dx_2 dx_3 \int_0^\infty b_1 db_1 b_2 db_2 \phi_B(x_1, b_1) \phi_\omega(x_2, b_2) \\ \times \{ [2x_3 r_\eta \phi_\eta^T(x_3, b_1) - x_3 \phi_\eta^A(x_3, b_1)] \\ \cdot \alpha_s(t_f) h_f(x_1, x_2, x_3, b_1, b_2) \exp[-S_{cd}(t_f)] \}, \quad (38)$$

$$M_e^{P1} = -\frac{32}{\sqrt{3}} G_F \pi C_F r_\omega m_B^4 \int_0^1 dx_1 dx_2 dx_3 \int_0^\infty b_1 db_1 b_2 db_2 \phi_B(x_1, b_1) \\ \cdot \{ [x_2 \phi_\eta^A(x_3, b_1) (\phi_\omega^s(x_2, b_2) - \phi_\omega^t(x_2, b_2)) + r_\eta ((x_2 + x_3) (\phi_\eta^P(x_3, b_1) \\ \cdot \phi_\omega^s(x_2, b_2) + \phi_\eta^T(x_3, b_1) \phi_\omega^t(x_2, b_2)) + (x_3 - x_2) (\phi_\eta^P(x_3, b_1) \phi_\omega^t(x_2, b_2) \\ + \phi_\eta^T(x_3, b_1) \phi_\omega^s(x_2, b_2)))] \alpha_s(t_f) h_f(x_1, x_2, x_3, b_1, b_2) \exp[-S_{cd}(t_f)] \} . \quad (39)$$

For the non-factorizable annihilation diagrams 1(e) and 1(f), there are three kinds of decay amplitudes. For the $(V - A)(V - A)$ operators, the decay amplitude M_a is

$$M_a = \frac{16}{\sqrt{3}} \pi G_F C_F m_B^4 \int_0^1 dx_1 dx_2 dx_3 \int_0^\infty b_1 db_1 b_2 db_2 \phi_B(x_1, b_1) \\ \cdot \{ [r_\omega r_\eta (x_3 - x_2) [\phi_\eta^P(x_3, b_2) \phi_\omega^t(x_2, b_2) + \phi_\eta^T(x_3, b_2) \phi_\omega^s(x_2, b_2)] \\ + r_\omega r_\eta (x_2 + x_3) [\phi_\eta^P(x_3, b_2) \phi_\omega^s(x_2, b_2) + \phi_\eta^T(x_3, b_2) \phi_\omega^t(x_2, b_2)] \\ + x_3 \phi_\omega(x_2, b_2) \phi_\eta^A(x_3, b_2)] \cdot \alpha_s(t_f^4) h_f^4(x_1, x_2, x_3, b_1, b_2) \exp[-S_{ef}(t_f^4)] \\ - [r_\omega r_\eta (x_2 - x_3) [\phi_\eta^P(x_3, b_2) \phi_\omega^t(x_2, b_2) + \phi_\eta^T(x_3, b_2) \phi_\omega^s(x_2, b_2)] \\ + r_\omega r_\eta [(2 + x_2 + x_3) \phi_\eta^P(x_3, b_2) \phi_\omega^s(x_2, b_2) - (2 - x_2 - x_3) \phi_\eta^T(x_3, b_2) \phi_\omega^t(x_2, b_2)] \\ + x_2 \phi_\omega(x_2, b_2) \phi_\eta^A(x_3, b_2)] \cdot \alpha_s(t_f^3) h_f^3(x_1, x_2, x_3, b_1, b_2) \exp[-S_{ef}(t_f^3)] \} . \quad (40)$$

For the $(V - A)(V + A)$ and $(S - P)(S + P)$ operators, we have

$$M_a^{P1} = \frac{16}{\sqrt{3}} G_F \pi C_F m_B^4 \int_0^1 dx_1 dx_2 dx_3 \int_0^\infty b_1 db_1 b_2 db_2 \phi_B(x_1, b_1) \\ \cdot \{ [x_2 r_\omega \phi_\eta^A(x_3, b_2) (\phi_\omega^s(x_2, b_2) + \phi_\omega^t(x_2, b_2)) - x_3 r_\eta (\phi_\eta^P(x_3, b_2) + \phi_\eta^T(x_3, b_2)) \\ \cdot \phi_\omega(x_2, b_2)] \cdot \alpha_s(t_f^4) h_f^4(x_1, x_2, x_3, b_1, b_2) \exp[-S_{ef}(t_f^4)] \\ + [(2 - x_2) r_\omega \phi_\eta^A(x_3, b_2) (\phi_\omega^s(x_2, b_2) + \phi_\omega^t(x_2, b_2)) - (2 - x_3) r_\eta (\phi_\eta^P(x_3, b_2) \\ + \phi_\eta^T(x_3, b_2)) \phi_\omega(x_2, b_2)] \cdot \alpha_s(t_f^3) h_f^3(x_1, x_2, x_3, b_1, b_2) \exp[-S_{ef}(t_f^3)] \} , \quad (41)$$

$$M_a^{P2} = -\frac{16}{\sqrt{3}} \pi G_F C_F m_B^4 \int_0^1 dx_1 dx_2 dx_3 \int_0^\infty b_1 db_1 b_2 db_2 \phi_B(x_1, b_1) \\ \cdot \{ [x_2 \phi_\omega(x_2, b_2) \phi_\eta^A(x_3, b_2) + r_\omega r_\eta ((x_2 - x_3) (\phi_\eta^P(x_3, b_2) \phi_\omega^t(x_2, b_2) + \phi_\eta^T(x_3, b_2) \\ \cdot \phi_\omega^s(x_2, b_2)) + (x_2 + x_3) (\phi_\eta^P(x_3, b_2) \phi_\omega^s(x_2, b_2) + \phi_\eta^T(x_3, b_2) \phi_\omega^t(x_2, b_2)))] \\ \cdot \alpha_s(t_f^4) h_f^4(x_1, x_2, x_3, b_1, b_2) \exp[-S_{ef}(t_f^4)] \\ - [x_3 \phi_\omega(x_2, b_2) \phi_\eta^A(x_3, b_2) + r_\omega r_\eta ((x_3 - x_2) (\phi_\eta^P(x_3, b_2) \phi_\omega^t(x_2, b_2) + \phi_\eta^T(x_3, b_2) \\ \cdot \phi_\omega^s(x_2, b_2)) + (2 + x_2 + x_3) \phi_\eta^P(x_3, b_2) \phi_\omega^s(x_2, b_2) - (2 - x_2 - x_3) \phi_\eta^T(x_3, b_2) \\ \cdot \phi_\omega^t(x_2, b_2))] \cdot \alpha_s(t_f^3) h_f^3(x_1, x_2, x_3, b_1, b_2) \exp[-S_{ef}(t_f^3)] \} . \quad (42)$$

The factorizable annihilation diagrams 1(g) and 1(h) involve only η and ω wave functions. There are also three kinds of decay amplitudes: F_a is for $(V - A)(V - A)$ type operators, F_a^{P1} and F_a^{P2} is for $(V - A)(V + A)$ and $(S - P)(S + P)$ type operators, respectively:

$$\begin{aligned}
F_a &= -F_a^{P1} \\
&= -4\sqrt{2}G_F\pi C_F m_B^4 \int_0^1 dx_2 dx_3 \int_0^\infty b_2 db_2 b_3 db_3 \{ [x_3 \phi_\eta^A(x_3, b_3) \phi_\omega(x_2, b_2) \\
&\quad + 2r_\omega r_\eta ((x_3 + 1) \phi_\eta^P(x_3, b_3) + (x_3 - 1) \phi_\eta^t(x_3, b_3)) \phi_\omega^s(x_2, b_2)] \\
&\quad \cdot \alpha_s(t_e^3) h_a(x_2, x_3, b_2, b_3) \exp[-S_{gh}(t_e^3)] \\
&\quad - [x_2 \phi_\eta^A(x_3, b_3) \phi_\omega(x_2, b_2) \\
&\quad + 2r_\eta r_\omega ((x_2 + 1) \phi_\omega^s(x_2, b_2) + (x_2 - 1) \phi_\omega^t(x_2, b_2)) \phi_\eta^P(x_3, b_3)] \\
&\quad \cdot \alpha_s(t_e^4) h_a(x_3, x_2, b_3, b_2) \exp[-S_{gh}(t_e^4)] \} , \tag{43}
\end{aligned}$$

$$\begin{aligned}
F_a^{P2} &= -8\sqrt{2}G_F\pi C_F m_B^4 \int_0^1 dx_2 dx_3 \int_0^\infty b_2 db_2 b_3 db_3 \\
&\quad \times \{ [x_3 r_\eta (\phi_\eta^P(x_3, b_3) - \phi_\eta^t(x_3, b_3)) \phi_\omega(x_2, b_2) + 2r_\omega \phi_\eta^A(x_3, b_3) \phi_\omega^s(x_2, b_2)] \\
&\quad \cdot \alpha_s(t_e^3) h_a(x_2, x_3, b_2, b_3) \exp[-S_{gh}(t_e^3)] \\
&\quad + [x_2 r_\omega (\phi_\omega^s(x_2, b_2) - \phi_\omega^t(x_2, b_2)) \phi_\eta^A(x_3, b_3) + 2r_\eta \phi_\omega(x_2, b_2) \phi_\eta^P(x_3, b_3)] \\
&\quad \cdot \alpha_s(t_e^4) h_a(x_3, x_2, b_3, b_2) \exp[-S_{gh}(t_e^4)] \} . \tag{44}
\end{aligned}$$

In the above equations, we have assumed that $x_1 \ll (x_2, x_3)$. Since the light quark momentum fraction x_1 in the B meson is peaked at the small region, while quark momentum fraction x_3 of η is peaked around 0.5, this is not a bad approximation. The numerical results also show that this approximation makes very little difference in the final result.

By exchanging the position of $\eta^{(\prime)}$ and ω in Fig. (1), one finds the new Feynman diagrams are illustrated in Fig. (2). Just like the case of Fig. (1), we firstly consider the factorizable diagrams 2(a) and 2(b). The decay amplitude F_e induced by inserting the $(V - A)(V - A)$ operators is

$$\begin{aligned}
F_{e\omega} &= 4\sqrt{2}G_F\pi C_F m_B^4 \int_0^1 dx_1 dx_3 \int_0^\infty b_1 db_1 b_3 db_3 \phi_B(x_1, b_1) \\
&\quad \cdot \{ [(1 + x_3) \phi_\omega(x_3, b_3) + (1 - 2x_3) r_\omega (\phi_\omega^s(x_3, b_3) + \phi_\omega^t(x_3, b_3))] \\
&\quad \cdot \alpha_s(t_e^1) h_e(x_1, x_3, b_1, b_3) \exp[-S_{ab}(t_e^1)] \\
&\quad + 2r_\omega \phi_\omega^s(x_3, b_3) \cdot \alpha_s(t_e^2) h_e(x_3, x_1, b_3, b_1) \exp[-S_{ab}(t_e^2)] \} , \tag{45}
\end{aligned}$$

The Fig. 2(a) and 2(b) are also the diagrams being used to extract the form factor $A_0^{B \rightarrow \omega}$. According the definition in Ref. [25], we can extract $A_0^{B \rightarrow \omega}$ from Eq.(45).

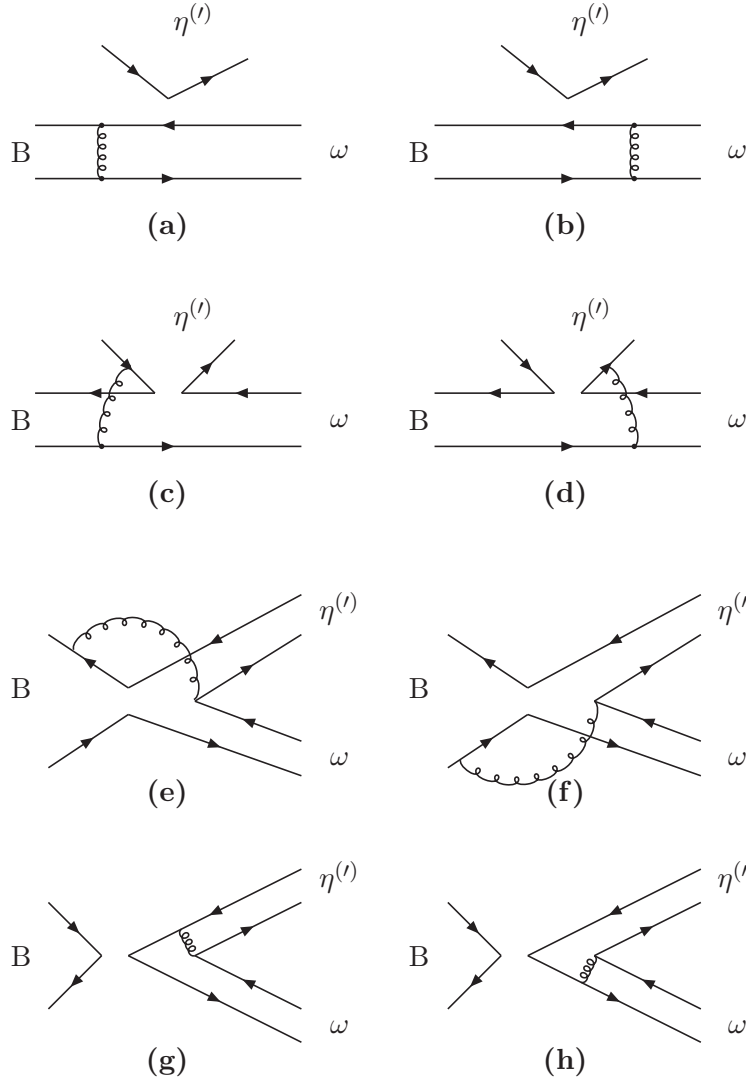


FIG. 2: Feynman diagrams contributing to the $B \rightarrow \omega \eta'$ decays when the ω boson picks up the spectator quark.

From Fig. 2(a) and 2(b), it is easy to find the decay amplitude $F_{e\omega}^{P1}$ and $F_{e\omega}^{P2}$:

$$F_{e\omega}^{P1} = -F_{e\omega}, \quad (46)$$

$$F_{e\omega}^{P2} = 8\sqrt{2}G_F\pi C_F r_\eta m_B^4 \int_0^1 dx_1 dx_3 \int_0^\infty b_1 db_1 b_3 db_3 \phi_B(x_1, b_1) \cdot \{ [\phi_\omega(x_3, b_3) + r_\omega((x_3 + 2)\phi_\omega^s(x_3, b_3) - x_3\phi_\omega^t(x_3, b_3))] \cdot \alpha_s(t_e^1) h_e(x_1, x_3, b_1, b_3) \exp[-S_{ab}(t_e^1)] + (x_1\phi_\omega(x_3, b_3) + 2r_\omega\phi_\omega^s(x_3, b_3)) \alpha_s(t_e^2) h_e(x_3, x_1, b_3, b_1) \exp[-S_{ab}(t_e^2)] \} . \quad (47)$$

For the non-factorizable diagrams 2(c) and 2(d), the corresponding decay amplitudes are

$$M_{e\omega} = -\frac{16}{\sqrt{3}}G_F\pi C_F m_B^4 \int_0^1 dx_1 dx_2 dx_3 \int_0^\infty b_1 db_1 b_2 db_2 \phi_B(x_1, b_1) \phi_\eta^A(x_2, b_2) \cdot \{ x_3 [\phi_\omega(x_3, b_1) - 2r_\omega\phi_\omega^t(x_3, b_1)] \alpha_s(t_f) h_f(x_1, x_2, x_3, b_1, b_2) \exp[-S_{cd}(t_f)] \} , \quad (48)$$

and

$$M_{e\omega}^{P1} = 0, \quad M_{e\omega}^{P2} = M_{e\omega}. \quad (49)$$

For the non-factorizable annihilation diagrams 2(e) and 2(f), again all three wave functions are involved. the three kinds of decay amplitudes are of the form

$$\begin{aligned} M_{a\omega} = & \frac{16}{\sqrt{3}} G_F \pi C_F m_B^4 \int_0^1 dx_1 dx_2 dx_3 \int_0^\infty b_1 db_1 b_2 db_2 \phi_B(x_1, b_1) \\ & \cdot \left\{ [x_3 \phi_\omega(x_3, b_2) \phi_\eta^A(x_2, b_2) + r_\omega r_\eta ((x_3 - x_2) (\phi_\eta^P(x_2, b_2) \phi_\omega^t(x_3, b_2) + \phi_\eta^T(x_2, b_2) \right. \\ & \cdot \phi_\omega^s(x_3, b_2)) + (x_3 + x_2) (\phi_\eta^P(x_2, b_2) \phi_\omega^s(x_3, b_2) + \phi_\eta^T(x_2, b_2) \phi_\omega^t(x_3, b_2))] \\ & \cdot \alpha_s(t_f^4) h_f^4(x_1, x_2, x_3, b_1, b_2) \exp[-S_{ef}(t_f^4)] - [x_2 \phi_\omega(x_3, b_2) \phi_\eta^A(x_2, b_2) \\ & + r_\omega r_\eta ((x_2 - x_3) (\phi_\eta^P(x_2, b_2) \phi_\omega^t(x_3, b_2) + \phi_\eta^T(x_2, b_2) \phi_\omega^s(x_3, b_2)) + r_\omega r_\eta \\ & \cdot ((2 + x_2 + x_3) \phi_\eta^P(x_2, b_2) \phi_\omega^s(x_3, b_2) - (2 - x_2 - x_3) \phi_\eta^T(x_2, b_2) \phi_\omega^t(x_3, b_2))] \\ & \cdot \alpha_s(t_f^3) h_f^3(x_1, x_2, x_3, b_1, b_2) \exp[-S_{ef}(t_f^3)] \} , \end{aligned} \quad (50)$$

$$\begin{aligned} M_{a\omega}^{P1} = & -\frac{16}{\sqrt{3}} G_F \pi C_F m_B^4 \int_0^1 dx_1 dx_2 dx_3 \int_0^\infty b_1 db_1 b_2 db_2 \phi_B(x_1, b_1) \\ & \cdot \left\{ [x_2 r_\eta \phi_\omega(x_3, b_2) (\phi_\eta^P(x_2, b_2) + \phi_\eta^T(x_2, b_2)) - x_3 r_\omega (\phi_\omega^s(x_3, b_2) + \phi_\omega^t(x_3, b_2)) \right. \\ & \cdot \phi_\eta^A(x_2, b_2)] \cdot \alpha_s(t_f^4) h_f^4(x_1, x_2, x_3, b_1, b_2) \exp[-S_{ef}(t_f^4)] \\ & + [(2 - x_2) r_\eta \phi_\omega(x_3, b_2) (\phi_\eta^P(x_2, b_2) + \phi_\eta^T(x_2, b_2)) - (2 - x_3) r_\omega (\phi_\omega^s(x_3, b_2) \\ & + \phi_\omega^t(x_3, b_2)) \phi_\eta^A(x_2, b_2)] \cdot \alpha_s(t_f^3) h_f^3(x_1, x_2, x_3, b_1, b_2) \exp[-S_{ef}(t_f^3)] \} , \end{aligned} \quad (51)$$

$$\begin{aligned} M_{a\omega}^{P2} = & -\frac{16}{\sqrt{3}} \pi G_F C_F m_B^4 \int_0^1 dx_1 dx_2 dx_3 \int_0^\infty b_1 db_1 b_2 db_2 \phi_B(x_1, b_1) \\ & \cdot \left\{ [x_2 \phi_\omega(x_3, b_2) \phi_\eta^A(x_2, b_2) + r_\omega r_\eta ((x_2 - x_3) (\phi_\eta^P(x_2, b_2) \phi_\omega^t(x_3, b_2) + \phi_\eta^T(x_2, b_2) \right. \\ & \cdot \phi_\omega^s(x_3, b_2)) + (x_2 + x_3) (\phi_\eta^P(x_2, b_2) \phi_\omega^s(x_3, b_2) + \phi_\eta^T(x_2, b_2) \phi_\omega^t(x_3, b_2))] \\ & \cdot \alpha_s(t_f^4) h_f^4(x_1, x_2, x_3, b_1, b_2) \exp[-S_{ef}(t_f^4)] \\ & - [x_3 \phi_\omega(x_3, b_2) \phi_\eta^A(x_2, b_2) + r_\omega r_\eta ((x_3 - x_2) (\phi_\eta^P(x_2, b_2) \phi_\omega^t(x_3, b_2) + \phi_\eta^T(x_2, b_2) \right. \\ & \cdot \phi_\omega^s(x_3, b_2)) + (2 + x_2 + x_3) \phi_\eta^P(x_2, b_2) \phi_\omega^s(x_3, b_2) - (2 - x_2 - x_3) \phi_\eta^T(x_2, b_2) \\ & \cdot \phi_\omega^t(x_3, b_2)] \cdot \alpha_s(t_f^3) h_f^3(x_1, x_2, x_3, b_1, b_2) \exp[-S_{ef}(t_f^3)] \} . \end{aligned} \quad (52)$$

For the factorizable annihilation diagrams 2(g) and 2(h), we have

$$F_{a\omega} = -F_a, \quad F_{a\omega}^{P1} = -F_a^{P1}, \quad F_{a\omega}^{P2} = -F_a^{P2}. \quad (53)$$

Following the same procedure, it is straightforward to calculate the decay amplitudes for the $B \rightarrow \phi \eta^{(\prime)}$ decays. It is worth of mentioning that all the eight Feynman diagrams in Fig. 1 after the replacements of the ω meson by the ϕ meson will contribute to $B \rightarrow \phi \eta^{(\prime)}$ decays; but Figs.2(a)-2(d) could not contribute to the same decay since $\phi = -s\bar{s}$ in the ideal mixing scheme of $\omega - \phi$ system.

Combining the contributions from the different diagrams, the total decay amplitude for $B^0 \rightarrow \omega\eta$ can be written as

$$\begin{aligned}
\sqrt{2}\mathcal{M}(\omega\eta) = & F_e F_1(\phi) f_\omega \left[\xi_u \left(C_1 + \frac{1}{3} C_2 \right) \right. \\
& - \xi_t \left(\frac{7}{3} C_3 + \frac{5}{3} C_4 + 2C_5 + \frac{2}{3} C_6 + \frac{1}{2} C_7 + \frac{1}{6} C_8 + \frac{1}{3} C_9 - \frac{1}{3} C_{10} \right) \Big] \\
& + M_e F_1(\phi) \left[\xi_u C_2 - \xi_t \left(C_3 + 2C_4 - 2C_6 - \frac{1}{2} C_8 - \frac{1}{2} C_9 + \frac{1}{2} C_{10} \right) \right] \\
& + F_{e\omega} \left[\xi_u \left(C_1 + \frac{1}{3} C_2 \right) f_\eta^d \right. \\
& - \xi_t \left(\frac{7}{3} C_3 + \frac{5}{3} C_4 - 2C_5 - \frac{2}{3} C_6 - \frac{1}{2} C_7 - \frac{1}{6} C_8 + \frac{1}{3} C_9 - \frac{1}{3} C_{10} \right) f_\eta^d \\
& - \xi_t \left(C_3 + \frac{1}{3} C_4 - C_5 - \frac{1}{3} C_6 + \frac{1}{2} C_7 + \frac{1}{6} C_8 - \frac{1}{2} C_9 - \frac{1}{6} C_{10} \right) f_\eta^s \Big] \\
& + F_{e\omega}^{P_2} \left[-\xi_t \left(\frac{1}{3} C_5 + C_6 - \frac{1}{6} C_7 - \frac{1}{2} C_8 \right) f_\eta^d \right] \\
& + M_{e\omega} F_1(\phi) \left[\xi_u C_2 - \xi_t \left(C_3 + 2C_4 + 2C_6 + \frac{1}{2} C_8 - \frac{1}{2} C_9 + \frac{1}{2} C_{10} \right) \right] \\
& + M_{e\omega} F_2(\phi) \left[-\xi_t \left(C_4 + C_6 - \frac{1}{2} C_8 - \frac{1}{2} C_{10} \right) \right] \\
& + (M_a + M_{a\omega}) F_1(\phi) \left[\xi_u C_2 - \xi_t \left(C_3 + 2C_4 - \frac{1}{2} C_9 + \frac{1}{2} C_{10} \right) \right] \\
& - (M_e^{P_1} + M_a^{P_1} + M_{a\omega}^{P_1}) F_1(\phi) \xi_t \left(C_5 - \frac{1}{2} C_7 \right) \\
& - (M_a^{P_2} + M_{a\omega}^{P_2}) F_1(\phi) \xi_t \left(2C_6 + \frac{1}{2} C_8 \right), \tag{54}
\end{aligned}$$

where $\xi_u = V_{ub}^* V_{ud}$, $\xi_t = V_{tb}^* V_{td}$, and

$$F_1(\phi) = \frac{\cos \phi}{\sqrt{2}}, \quad F_2(\phi) = -\sin \phi, \tag{55}$$

are the mixing factors. The Wilson coefficients $C_i = C_i(t)$ in Eq. (54) should be calculated at the appropriate scale t using equations as given in the Appendices of Ref. [19].

By doing the replacements of $f_\omega \rightarrow f_\phi$ and $\phi_\omega^{A,P,T} \rightarrow \phi_\phi^{A,P,T}$, one obtains the decay amplitude for $B^0 \rightarrow \phi\eta$ decay:

$$\begin{aligned}
\mathcal{M}(\phi\eta) = & F_e \xi_t \left(C_3 + \frac{1}{3} C_4 + C_5 + \frac{1}{3} C_6 - \frac{1}{2} C_7 - \frac{1}{6} C_8 - \frac{1}{2} C_9 - \frac{1}{6} C_{10} \right) F_1(\phi) \\
& + M_e \xi_t \left(C_4 - C_6 + \frac{1}{2} C_8 - \frac{1}{2} C_{10} \right) F_1(\phi) + (M_a + M_{a\phi}) \xi_t \left(C_4 - \frac{1}{2} C_{10} \right) F_2(\phi) \\
& + (M_a^{P_2} + M_{a\phi}^{P_2}) \xi_t \left(C_6 - \frac{1}{2} C_8 \right) F_2(\phi). \tag{56}
\end{aligned}$$

The complete decay amplitude $\mathcal{M}(\omega\eta')$ and $\mathcal{M}(\phi\eta')$ can be obtained easily from Eq.(54) and Eq.(56) by the following replacements

$$\begin{aligned} f_\eta^d, f_\eta^s &\longrightarrow f_{\eta'}^d, f_{\eta'}^s, \\ F_1(\phi) &\longrightarrow F_1'(\phi) = \frac{\sin\phi}{\sqrt{2}}, \\ F_2(\phi) &\longrightarrow F_2'(\phi) = \cos\phi. \end{aligned} \tag{57}$$

IV. NUMERICAL RESULTS AND DISCUSSIONS

In this section, we will present the numerical results of the branching ratios and CP violating asymmetries for those considered decay modes.

A. Input parameters

We show here the input parameters to be used in the numerical calculations. The masses, decay constants, QCD scale and B^0 meson lifetime are

$$\begin{aligned} \Lambda_{\overline{\text{MS}}}^{(f=4)} &= 250\text{MeV}, \quad f_\pi = 130\text{MeV}, \quad f_B = 190\text{MeV}, \\ f_\phi &= 237\text{MeV}, \quad f_\phi^T = 220\text{MeV}, \quad M_W = 80.41\text{GeV}, \\ f_\omega &= 195\text{MeV}, \quad f_\omega^T = 140\text{MeV}, \quad M_\phi = 1.02\text{GeV}, \\ M_\omega &= 0.78\text{GeV}, \quad m_\eta = 547.5\text{MeV}, \quad m_{\eta'} = 957.8\text{MeV}, \\ M_B &= 5.2792\text{GeV}, \quad \tau_{B^0} = 1.54 \times 10^{-12}\text{s}. \end{aligned} \tag{58}$$

For the Cabibbo-Kobayashi-Maskawa (CKM) matrix elements, here we adopt the Wolfenstein parametrization for the CKM matrix up to $\mathcal{O}(\lambda^5)$ with the parameters $\lambda = 0.2272$, $A = 0.818$, $\bar{\rho} = 0.221$ and $\bar{\eta} = 0.340$ [20].

From Eq.(45) we find the numerical values of the corresponding form factors at zero momentum transfer: $A_0^{B \rightarrow \omega}(q^2 = 0) = 0.35 \pm 0.05(\omega_b)$ which are consistent with those given in [32].

B. Branching ratios

For $B^0 \rightarrow \omega\eta^{(\prime)}$ and $\phi\eta^{(\prime)}$ decays, the decay amplitudes as given in Eqs. (54) and (56) can be rewritten as

$$\mathcal{M} = V_{ub}^* V_{ud} T - V_{tb}^* V_{td} P = V_{ub}^* V_{ud} T [1 + z e^{i(\alpha+\delta)}], \tag{59}$$

where

$$z = \left| \frac{V_{tb}^* V_{td}}{V_{ub}^* V_{ud}} \right| \left| \frac{P}{T} \right|, \quad \alpha = \arg \left[-\frac{V_{td} V_{tb}^*}{V_{ud} V_{ub}^*} \right] \tag{60}$$

are the ratio of penguin to tree contributions and the weak phase (one of the three CKM angles) respectively, and δ is the relative strong phase between tree (T) and penguin (P)

diagrams. The CP-averaged branching ratio for $B^0 \rightarrow \omega(\phi)\eta^{(\prime)}$ decays can be then written as

$$Br = (|\mathcal{M}|^2 + |\overline{\mathcal{M}}|^2)/2 = |V_{ub}V_{ud}^*T|^2 [1 + 2z \cos \alpha \cos \delta + z^2], \quad (61)$$

where the ratio z and the strong phase δ have been defined in Eqs.(59) and (60).

Using the wave functions and the input parameters as specified in previous sections, it is straightforward to calculate the branching ratios for the four considered decays. We find numerically that

$$Br(B^0 \rightarrow \omega\eta) = [2.7_{-0.6}^{+0.8}(\omega_b) \pm 0.7(\alpha) \pm 0.3(a_2)] \times 10^{-7}, \quad (62)$$

$$Br(B^0 \rightarrow \omega\eta') = [0.75_{-0.14}^{+0.19}(\omega_b)_{-0.24}^{+0.25}(\alpha)_{-0.17}^{+0.19}(a_2)] \times 10^{-7}, \quad (63)$$

The main errors are induced by the uncertainties of $\omega_b = 0.4 \pm 0.04$ GeV, $\alpha = 100^\circ \pm 20^\circ$ and $a_2 = 0.115 \pm 0.115$, respectively.

For the $B^0 \rightarrow \phi\eta^{(\prime)}$ decays, the decay amplitudes involve only the penguin (P) diagrams, the branching ratios are:

$$Br(B^0 \rightarrow \phi\eta) = [6.3_{-1.0}^{+1.2}(\omega_b)_{-1.0}^{+2.7}(m_s)_{-1.3}^{+1.4}(a_2)] \times 10^{-9}, \quad (64)$$

$$Br(B^0 \rightarrow \phi\eta') = [7.3_{-1.3}^{+1.5}(\omega_b)_{-0.9}^{+2.3}(m_s)_{-2.0}^{+2.2}(a_2)] \times 10^{-9}, \quad (65)$$

The main errors are induced by the uncertainties of $\omega_b = 0.4 \pm 0.04$ GeV, $m_s = 130 \pm 30$ MeV and $a_2 = 0.115 \pm 0.115$, respectively.

For the CP-averaged branching ratios of the considered four decays, the PQCD predictions agree within errors with both the experimental upper limits as shown in Eqs.(1-2), and the theoretical predictions in the QCDF approach, for example, as given in Ref. [1]:

$$Br(B^0 \rightarrow \omega\eta) = (0.31_{-0.27}^{+0.46}) \times 10^{-6}, \quad (66)$$

$$Br(B^0 \rightarrow \omega\eta') = (0.20_{-0.18}^{+0.34}) \times 10^{-6}, \quad (67)$$

$$Br(B^0 \rightarrow \phi\eta^{(\prime)}) \approx 1 \times 10^{-9}, \quad (68)$$

where the individual errors as given in Refs. [1] have been added in quadrature. It is easy to see that the central values of the pQCD predictions for $Br(B \rightarrow \phi\eta^{(\prime)})$ are larger than the corresponding QCDF predictions, although they are still consistent if the large theoretical uncertainties are taken into account. The branching ratios $Br(B \rightarrow \omega\eta^{(\prime)})$ at the 10^{-7} level can be measured in the forthcoming LHC experiments [33]. But it is very difficult to measure $B \rightarrow \phi\eta^{(\prime)}$ decays because of their tiny ($\sim 10^{-9}$) branching ratio, if the pQCD predictions are true.

It is worth stressing that the theoretical predictions in the pQCD approach have large theoretical errors induced by the still large uncertainties of many input parameters. In our analysis, we considered the constraints on these parameters from analysis of other well measured decay channels. From numerical calculations, we get to know that the main errors come from the uncertainty of ω_b , m_s , α and $a_2^{\eta_{q(s)}}$. Additionally, the final-state interactions remains unsettled in pQCD, which is non-perturbative in nature but not universal.

In Fig. 3 we show the parameter dependence of the pQCD predictions for the branching ratios of $B \rightarrow \omega\eta$ and $\omega\eta'$ decays for $\omega_b = 0.4 \pm 0.04$ GeV, $\alpha = [0^\circ, 180^\circ]$. From the numerical results and the figures we observe that the pQCD predictions are sensitive to the variations of ω_b and α .

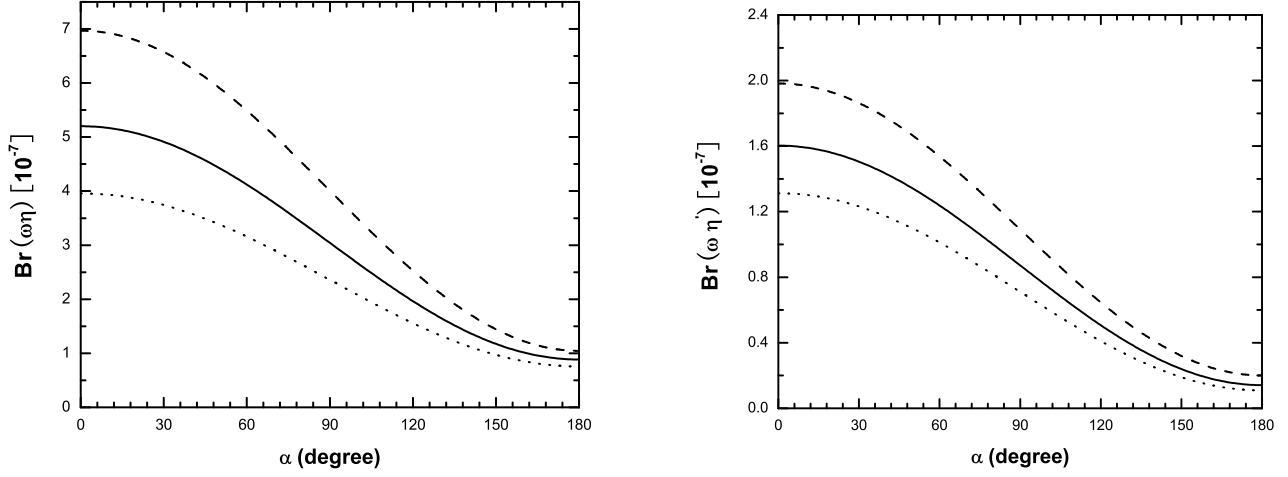


FIG. 3: The α dependence of the branching ratios (in unit of 10^{-7}) of $B^0 \rightarrow \omega\eta$ and $\omega\eta'$ decays for $\phi = 39.3^\circ$, $\omega_b = 0.36$ GeV (dashed curve), 0.40 GeV (solid curve) and 0.44 GeV (dotted curve).

C. CP-violating asymmetries

Now we turn to the evaluations of the CP-violating asymmetries of $B \rightarrow \omega\eta^{(\prime)}$ decays in pQCD approach. Because these decays are neutral B meson decays, so we should consider the effects of $B^0 - \bar{B}^0$ mixing. For B^0 meson decays into a CP eigenstate f , the time-dependent CP-violating asymmetry can be defined as

$$\frac{Br(\bar{B}^0(t) \rightarrow f) - Br(B^0(t) \rightarrow f)}{Br(\bar{B}^0(t) \rightarrow f) + Br(B^0(t) \rightarrow f)} \equiv \mathcal{A}_{CP}^{dir} \cos(\Delta m t) + \mathcal{A}_{CP}^{mix} \sin(\Delta m t), \quad (69)$$

where Δm is the mass difference between the two B_d^0 mass eigenstates, $t = t_{CP} - t_{tag}$ is the time difference between the tagged B^0 (\bar{B}^0) and the accompanying \bar{B}^0 (B^0) with opposite b flavor decaying to the final CP-eigenstate f_{CP} at the time t_{CP} . The direct and mixing induced CP-violating asymmetries \mathcal{A}_{CP}^{dir} and \mathcal{A}_{CP}^{mix} can be written as

$$\mathcal{A}_{CP}^{dir} = \frac{|\lambda_{CP}|^2 - 1}{1 + |\lambda_{CP}|^2}, \quad \mathcal{A}_{CP}^{mix} = \frac{2Im(\lambda_{CP})}{1 + |\lambda_{CP}|^2}, \quad (70)$$

where the CP-violating parameter λ_{CP} is

$$\lambda_{CP} = \frac{V_{tb}^* V_{td} \langle f | H_{eff} | \bar{B}^0 \rangle}{V_{tb} V_{td}^* \langle f | H_{eff} | B^0 \rangle} = e^{2i\alpha} \frac{1 + ze^{i(\delta-\alpha)}}{1 + ze^{i(\delta+\alpha)}}. \quad (71)$$

Here the ratio z and the strong phase δ have been defined previously. In pQCD approach, since both z and δ are calculable, it is easy to find the numerical values of \mathcal{A}_{CP}^{dir} and \mathcal{A}_{CP}^{mix} for the considered decay processes.

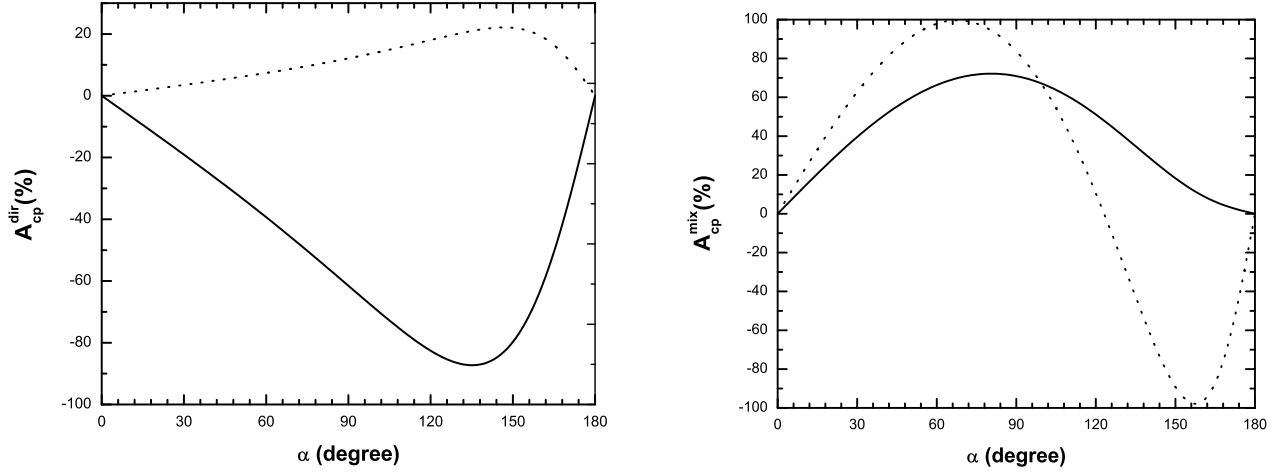


FIG. 4: The direct and mixing-induced CP asymmetry (in percentage) of $B^0 \rightarrow \omega\eta$ (solid curve) and $\omega\eta'$ (dotted curve) decay as a function of CKM angle α .

By using the central values of the input parameters, one found the pQCD predictions (in unit of 10^{-2}) for the direct and mixing induced CP-violating asymmetries of the considered decays

$$\mathcal{A}_{CP}^{dir}(B^0 \rightarrow \omega\eta) = -69.1_{-13.4}^{+15.1}(\alpha), \quad \mathcal{A}_{CP}^{mix}(B^0 \rightarrow \omega\eta) = +66.9_{-15.8}^{+5.3}(\alpha), \quad (72)$$

$$\mathcal{A}_{CP}^{dir}(B^0 \rightarrow \omega\eta') = +13.9_{-3.5}^{+4.1}(\alpha), \quad \mathcal{A}_{CP}^{mix}(B^0 \rightarrow \omega\eta') = +65.8_{-55.2}^{+29.1}(\alpha), \quad (73)$$

where the dominant errors come from the variations of $\alpha = 100^\circ \pm 20^\circ$.

In Fig. 4, we show the α -dependence of the pQCD predictions for the direct and the mixing-induced CP-violating asymmetry for $B^0 \rightarrow \omega\eta$ (solid curve) and $B^0 \rightarrow \omega\eta'$ (dotted curve) decay, respectively. The pQCD predictions in Eqs. (72,73) are consistent with the QCDF predictions due to very large uncertainties in the QCDF approach [1].

If we integrate the time variable t , we will get the total CP asymmetry for $B^0 \rightarrow \omega\eta^{(\prime)}$ decays (in units of 10^{-2}):

$$\mathcal{A}_{CP}^{tot}(B^0 \rightarrow \omega\eta) = -11_{-15.1}^{+12.1}(\alpha), \quad (74)$$

$$\mathcal{A}_{CP}^{tot}(B^0 \rightarrow \omega\eta') = +40.6_{-24.2}^{+11.8}(\alpha). \quad (75)$$

For the $B^0 \rightarrow \phi\eta^{(\prime)}$ decay modes, however, there is no CP asymmetry, the reason is that they involve only penguin contributions and one type of CKM elements.

It is worth of mentioning that although the CP-violating asymmetries of $B \rightarrow \omega\eta^{(\prime)}$ decays are rather large in size, but it may be difficult to measure them because of the predicted small branching ratios at 10^{-7} level [33].

D. Effects of possible gluonic component of η'

Up to now, we have not considered the possible contributions to the branching ratios and CP-violating asymmetries of $B \rightarrow \omega(\phi)\eta^{(\prime)}$ decays induced by the possible gluonic component of η and η' meson. For η meson, one generally believe that its gluonic component is negligibly small. For η' meson, however, a large gluonic component is generally expected because of the observed very large $B \rightarrow K\eta'$ branching ratio.

When a non-zero gluonic component exist in η' meson, an additional decay amplitude \mathcal{M}' will be produced. Such decay amplitude may construct or destruct with the ones from the $q\bar{q}$ ($q = u, d, s$) components of η' , the branching ratios of the decays in question may be increased or decreased accordingly.

In Ref. [9], by employing the pQCD factorization approach, Charng, Kurimoto and Li calculated the flavor-singlet contribution to the $B \rightarrow \eta^{(\prime)}$ transition form factors induced by the Feynman diagrams with the two gluons emitted from the light quark of the B meson (see Fig. 1 of Ref. [9]), the dominant gluonic contribution is negligible for $B \rightarrow \eta$ form factor, and also small (less than 5%) for the $B \rightarrow \eta'$ ones [13].

Following the procedure of Ref. [9] and using the formulae given there, we also calculate the gluonic contributions to $B \rightarrow \omega(\phi)\eta'$ decays. If we add the gluonic contribution to the form factor $F_0^{B \rightarrow \eta'}$ but keeping all other inputs in their default central values, we find numerically that

$$Br(B^0 \rightarrow \omega\eta') = 0.82 \times 10^{-7}, \quad (76)$$

$$Br(B^0 \rightarrow \phi\eta') = 6.5 \times 10^{-9}. \quad (77)$$

One can see that the variation of the central values of the pQCD predictions induced by the inclusion of gluonic contribution is only about $\pm 10\%$, much smaller than the theoretical uncertainties from the variations of input parameters ω_b , m_s , or α .

V. SUMMARY

In this paper, we calculated the branching ratios of $B^0 \rightarrow \omega\eta^{(\prime)}$, $\phi\eta^{(\prime)}$ decays and CP-violating asymmetries of $B^0 \rightarrow \omega\eta^{(\prime)}$ decays at the leading order by using the pQCD factorization approach.

Besides the usual factorizable diagrams, the non-factorizable and annihilation diagrams are also calculated analytically. Although the non-factorizable and annihilation contributions are sub-leading for the branching ratios of the considered decays, but they are not negligible. Furthermore these diagrams provide the necessary strong phase required by a non-zero CP-violating asymmetry for the considered decays.

After calculating all the diagrams, we found the branching ratios of the four related decays are very small, $Br(B \rightarrow \omega\eta^{(\prime)})$ are at the order of $O(10^{-7})$ and $Br(B \rightarrow \phi\eta^{(\prime)})$ are around 10^{-9} . We also predict the direct and mixing-induced CP asymmetries of the $B \rightarrow \omega\eta^{(\prime)}$. Moreover, we compare our results with the current experimental data and the theoretical predictions in QCDF approach. In short, we found that

- For the CP-averaged branching ratios of the considered decay modes, the pQCD

predictions are

$$Br(B^0 \rightarrow \omega\eta) = (2.7_{-1.0}^{+1.1}) \times 10^{-7}, \quad (78)$$

$$Br(B^0 \rightarrow \omega\eta') = (0.75_{-0.33}^{+0.37}) \times 10^{-7}, \quad (79)$$

$$Br(B^0 \rightarrow \phi\eta) = (6.3_{-1.9}^{+3.3}) \times 10^{-9}, \quad (80)$$

$$Br(B^0 \rightarrow \phi\eta') = (7.3_{-2.6}^{+3.5}) \times 10^{-9}, \quad (81)$$

where the various errors as specified in Eqs. (62)-(65) have been added in quadrature. The inclusion of the gluonic contribution can change the branching ratios of $B \rightarrow \omega\eta', \phi\eta'$ decays by about 10% in magnitude.

- The pQCD predictions for the CP-violating asymmetries of $B \rightarrow \omega\eta^{(\prime)}$ decays are large in size.
- The major theoretical errors are induced by the uncertainties of the input parameters ω_B , the mass m_s , the CKM angle α and the Gegenbauer moment $a_2^{\eta_{q(s)}}$.

Acknowledgments

We are very grateful to Cai-Dian Lü, Ying Li, Xin Liu and Huisheng Wang for helpful discussions. This work is partly supported by the National Natural Science Foundation of China under Grant No.10575052, and by the Specialized Research Fund for the doctoral Program of higher education (SRFDP) under Grant No. 20050319008.

APPENDIX A: RELATED FUNCTIONS

We show here the function h_i appearing in the expressions of the decay amplitudes in section III, coming from the Fourier transformations of the function $H^{(0)}$,

$$h_e(x_1, x_3, b_1, b_3) = K_0(\sqrt{x_1 x_3} m_B b_1) [\theta(b_1 - b_3) K_0(\sqrt{x_3} m_B b_1) I_0(\sqrt{x_3} m_B b_3) + \theta(b_3 - b_1) K_0(\sqrt{x_3} m_B b_3) I_0(\sqrt{x_3} m_B b_1)] S_t(x_3), \quad (A1)$$

$$h_a(x_2, x_3, b_2, b_3) = K_0(i\sqrt{x_2 x_3} m_B b_2) [\theta(b_3 - b_2) K_0(i\sqrt{x_3} m_B b_3) I_0(i\sqrt{x_3} m_B b_2) + \theta(b_2 - b_3) K_0(i\sqrt{x_3} m_B b_2) I_0(i\sqrt{x_3} m_B b_3)] S_t(x_3), \quad (A2)$$

$$h_f(x_1, x_2, x_3, b_1, b_2) = \left\{ \theta(b_2 - b_1) I_0(M_B \sqrt{x_1 x_3} b_1) K_0(M_B \sqrt{x_1 x_3} b_2) + (b_1 \leftrightarrow b_2) \right\} \cdot \left(\begin{array}{ll} K_0(M_B F_{(1)} b_2), & \text{for } F_{(1)}^2 > 0 \\ \frac{\pi i}{2} H_0^{(1)}(M_B \sqrt{|F_{(1)}^2|} b_2), & \text{for } F_{(1)}^2 < 0 \end{array} \right), \quad (A3)$$

$$h_f^3(x_1, x_2, x_3, b_1, b_2) = \left\{ \theta(b_1 - b_2) K_0(i\sqrt{x_2 x_3} b_1 M_B) I_0(i\sqrt{x_2 x_3} b_2 M_B) + (b_1 \leftrightarrow b_2) \right\} \cdot K_0(\sqrt{x_1 + x_2 + x_3 - x_1 x_3 - x_2 x_3} b_1 M_B), \quad (A4)$$

$$h_f^4(x_1, x_2, x_3, b_1, b_2) = \left\{ \theta(b_1 - b_2) K_0(i\sqrt{x_2 x_3} b_1 M_B) I_0(i\sqrt{x_2 x_3} b_2 M_B) \right. \\ \left. + (b_1 \leftrightarrow b_2) \right\} \cdot \left(\begin{array}{ll} K_0(M_B F_{(2)} b_1), & \text{for } F_{(2)}^2 > 0 \\ \frac{\pi i}{2} H_0^{(1)}(M_B \sqrt{|F_{(2)}^2|} b_1), & \text{for } F_{(2)}^2 < 0 \end{array} \right), \quad (\text{A5})$$

where J_0 is the Bessel function, K_0 and I_0 are the modified Bessel functions $K_0(-ix) = -(\pi/2)Y_0(x) + i(\pi/2)J_0(x)$, $H_0^{(1)}(z) = J_0(z) + iY_0(z)$, and the $F_{(j)}$ are defined by

$$F_{(1)}^2 = (x_1 - x_2)x_3, \quad (\text{A6})$$

$$F_{(2)}^2 = (x_1 - x_2)x_3. \quad (\text{A7})$$

The threshold resummation form factor $S_t(x_i)$ is adopted from Ref. [24]

$$S_t(x) = \frac{2^{1+2c}\Gamma(3/2+c)}{\sqrt{\pi}\Gamma(1+c)}[x(1-x)]^c, \quad (\text{A8})$$

where the parameter $c = 0.3$. This function is normalized to unity.

The Sudakov factors appearing in section III are defined as

$$S_{ab}(t) = s\left(x_1 m_B/\sqrt{2}, b_1\right) + s\left(x_3 m_B/\sqrt{2}, b_3\right) + s\left((1-x_3)m_B/\sqrt{2}, b_3\right) \\ - \frac{1}{\beta_1} \left[\ln \frac{\ln(t/\Lambda)}{-\ln(b_1\Lambda)} + \ln \frac{\ln(t/\Lambda)}{-\ln(b_3\Lambda)} \right], \quad (\text{A9})$$

$$S_{cd}(t) = s\left(x_1 m_B/\sqrt{2}, b_1\right) + s\left(x_2 m_B/\sqrt{2}, b_2\right) + s\left((1-x_2)m_B/\sqrt{2}, b_2\right) \\ + s\left(x_3 m_B/\sqrt{2}, b_1\right) + s\left((1-x_3)m_B/\sqrt{2}, b_1\right) \\ - \frac{1}{\beta_1} \left[2 \ln \frac{\ln(t/\Lambda)}{-\ln(b_1\Lambda)} + \ln \frac{\ln(t/\Lambda)}{-\ln(b_2\Lambda)} \right], \quad (\text{A10})$$

$$S_{ef}(t) = s\left(x_1 m_B/\sqrt{2}, b_1\right) + s\left(x_2 m_B/\sqrt{2}, b_2\right) + s\left((1-x_2)m_B/\sqrt{2}, b_2\right) \\ + s\left(x_3 m_B/\sqrt{2}, b_2\right) + s\left((1-x_3)m_B/\sqrt{2}, b_2\right) \\ - \frac{1}{\beta_1} \left[\ln \frac{\ln(t/\Lambda)}{-\ln(b_1\Lambda)} + 2 \ln \frac{\ln(t/\Lambda)}{-\ln(b_2\Lambda)} \right], \quad (\text{A11})$$

$$S_{gh}(t) = s\left(x_2 m_B/\sqrt{2}, b_2\right) + s\left(x_3 m_B/\sqrt{2}, b_3\right) + s\left((1-x_2)m_B/\sqrt{2}, b_2\right) \\ + s\left((1-x_3)m_B/\sqrt{2}, b_3\right) - \frac{1}{\beta_1} \left[\ln \frac{\ln(t/\Lambda)}{-\ln(b_2\Lambda)} + \ln \frac{\ln(t/\Lambda)}{-\ln(b_3\Lambda)} \right], \quad (\text{A12})$$

where the function $s(q, b)$ are defined in the Appendix A of Ref. [19]. The scale t_i 's in the

above equations are chosen as

$$\begin{aligned}
t_e^1 &= \max(\sqrt{x_3}m_B, 1/b_1, 1/b_3) , \\
t_e^2 &= \max(\sqrt{x_1}m_B, 1/b_1, 1/b_3) , \\
t_e^3 &= \max(\sqrt{x_3}m_B, 1/b_2, 1/b_3) , \\
t_e^4 &= \max(\sqrt{x_2}m_B, 1/b_2, 1/b_3) , \\
t_f &= \max(\sqrt{x_1x_3}m_B, \sqrt{(x_1 - x_2)x_3}m_B, 1/b_1, 1/b_2) , \\
t_f^3 &= \max(\sqrt{x_1 + x_2 + x_3 - x_1x_3 - x_2x_3}m_B, \sqrt{x_2x_3}m_B, 1/b_1, 1/b_2) , \\
t_f^4 &= \max(\sqrt{x_2x_3}m_B, \sqrt{(x_1 - x_2)x_3}m_B, 1/b_1, 1/b_2) .
\end{aligned} \tag{A13}$$

They are given as the maximum energy scale appearing in each diagram to kill the large logarithmic radiative corrections.

-
- [1] M. Beneke and M. Neubert, Nucl. Phys. B **675**, 333 (2003); Nucl. Phys. B **651**, 225 (2003).
 - [2] M. Beneke, G. Buchalla, M. Neubert, and C.T. Sachrajda, Phys. Rev. Lett. **83**, 1914 (1999).
 - [3] H.N. Li and H.L. Yu, Phys. Rev. Lett. **74**, 4388 (1995); Phys. Lett. B **353**, 301 (1995); Phys. Rev. D **53**, 2480 (1996); Y.Y. Keum, H.N. Li and A.I. Sanda, Phys. Rev. D **63**, 054008 (2001).
 - [4] E. Kou and A.I. Sanda, Phys. Lett. B **525**, 240 (2002).
 - [5] X. Liu, H.S. Wang, Z.J. Xiao, L.B. Guo, and C.D. Lü, Phys. Rev. D **73**, 074002 (2006).
 - [6] H.S. Wang, X. Liu, Z.J. Xiao, L.B. Guo, and C.D. Lü, Nucl. Phys. B **738**, 243 (2006).
 - [7] Z.J. Xiao, D.Q. Guo, and X.F. Chen, Phys. Rev. D **75**, 014018 (2007).
 - [8] Z.J. Xiao, Xin Liu and H.S. Wang, Phys. Rev. D **75**, 034017 (2007); Z.J. Xiao, X.F. Chen and D.Q. Guo, Eur.Phys.J. C **50** (2007) in press (hep-ph/0608222); X.F. Chen, D.Q. Guo, and Z.J. Xiao, hep-ph/0701146.
 - [9] Y.Y. Charng, T. Kurimoto, and H.N. Li, Phys. Rev. D **74**, 074024 (2006).
 - [10] Heavy Flavor Averaging Group, E. Barberio *et al.*, hep-ex/0603003, updated in <http://www.slac.stanford.edu/xorg/hfag>.
 - [11] J. Schümann *et al.*, Belle Collaboration, hep-ex/0701046.
 - [12] A. Ali and A. Ya. Parkhomenko, Eur.Phys.J. C **30** 183 (2003).
 - [13] H.N. Li, lectures presented at Nanjing Normal University, P.R. China, Dec.4-5, 2006.
 - [14] C.-H. V. Chang and H.N. Li, Phys. Rev. D **55**, 5577 (1997); T.-W. Yeh and H.N. Li, Phys. Rev. D **56**, 1615 (1997); H.N. Li, Prog.Part.& Nucl.Phys. **51**, 85 (2003), and reference therein.
 - [15] G.P. Lepage and S.J. Brodsky, Phys. Rev. D **22**, 2157 (1980).
 - [16] S. Descotes-Genon and C.T. Sachrajda, Nucl. Phys. B **625**, 239 (2002); Z.T. Wei, M.Z. Yang, Nucl. Phys. B **642**, 263 (2002); M. Beneke and T. Feldmann, Nucl. Phys. B **685**, 249 (2004).
 - [17] H.N. Li and B. Tseng, Phys. Rev. D **57**, 443, (1998).
 - [18] For a review see G. Buchalla, A.J. Buras, and M.E. Lautenbacher, Rev. Mod. Phys. **68**, 1125 (1996).

- [19] C.D. Lü, K. Ukai, and M.Z. Yang, Phys. Rev. D **63**, 074009 (2001);
- [20] Particle Data Group, W.-M. Yao *et al.*, J. Phys. G **33**, 1 (2006).
- [21] T. Feldmann, P. Kroll and B. Stech, Phys. Rev. D **58**, 114006 (1998); Phys. Lett. B **449**, 339 (1999); T. Feldmann, Int. J. Mod. Phys. A **15**, 159 (2000).
- [22] R. Escribano and J.M. Frere, JHEP 0506 (2005) 029.
- [23] E. Kou, Phys. Rev. D **63**, 054027 (2001).
- [24] T. Kurimoto, H.N. Li, A.I. Sanda, Phys. Rev. D **65**, 014007 (2001).
- [25] C.D. Lü, M.Z. Yang, Eur.Phys.J. C **28**, 515 (2003).
- [26] P. Ball, J. High Energy Phys. 9809, (1998) 005; P. Ball, J. High Energy Phys. 9901, (1999) 010.
- [27] P. Ball and R. Zwicky, Phys. Rev. D **71**, 014015 (2005).
- [28] P. Ball, V.M. Braun, and A. Lenz, J. High Energy Phys. **0605** (2006) 004.
- [29] P. Ball, V.M. Braun, Y. Koike, and K. Tanaka, Nucl. Phys. B **529**, 323 (1998)
- [30] H.W. Huang, C.D. Lü, T. Morii, Y.L. Shen, G.L. Song, and J. Zhu, Phys. Rev. D **73**, 014011 (2006).
- [31] Y. Li, and C.D. Lü, Phys. Rev. D **73**, 014024 (2006).
- [32] P. Ball and R. Zwicky, Phys. Rev. D **71**, 014029 (2005).
- [33] P. Ball et al., B Decays at the LHC, CERN-TH-2000-101, in “Geneva 1999, Standard model physics (and more) at the LHC”, p305-417; hep-ph/0003238; T. Skwarnicki, talk presented at Aspen 2007, 8-13 Jan. 2007, Aspen, Colorado.